

Factors That Influence the Negative Corona Charging of Nonwoven Filter Media

Belaid Tabti,

Lucian Dascalescu

PPRIME Institute, UPR 3346 CNRS
University of Poitiers-ENSMA, France
btabti@ymail.com
lucian.dascalescu@univ-poitiers.fr

Marius Plopeanu,

Agela Antoniu

PPRIME Institute, UPR 3346 CNRS
University of Poitiers-ENSMA, France
marius.plopeanu@hotmail.com
avasilut@gmail.com

Belkacem Yahiaoui,

Ahmed Melahi

Laboratory of Electrical Engineering,
University of Bejaia, Algeria
Bel.yahiaoui@yahoo.fr
melahi_ahmed@yahoo.fr

Abstract -- The aim of this paper is to analyze the corona charging and charge decay of nonwoven fabrics, by using the surface potential decay (SPD) measurement techniques and its (tdV_s/dt) versus $(\log t)$ representation. Samples of nonwoven polypropylene (PP) fibrous media were exposed to negative corona discharges, using a triode-type electrode arrangement, energized from a DC high-voltage supply operating as a constant current generator. Using the above-mentioned mathematical transformation and varying some experimental conditions, it has been possible to identify the contribution of different physical mechanisms to the SPD. The effect of charge injection assisted by the negative corona as well as that of neutral excited species present in the discharge were clearly pointed out. The experiments demonstrated that the initial potential and the dynamic of the potential decay are substantially affected by the air humidity. Thermal conditioning improves the charging state of nonwoven fabrics.

Index Terms—Corona charging, nonwoven dielectric materials, polypropylene fibers, surface potential decay (SPD).

I. INTRODUCTION

Fibrous electret filters media consist of nonwoven fabrics made of dielectric materials that have a quasi-permanent electrical charge. Electric charging of the media improves their particle collection efficiency by the electrostatic particle capture mechanism that enhances the conventional mechanical filtration without causing an increase of the pressure drop [1]-[3]. The lifetime of electret filters depends on the rate of the charge decay, as the latter is accompanied by the decrease of collection efficiency.

Corona charging using a triode-type electrode arrangement has been extensively employed for the investigation of the charge dynamic characteristics of dielectric materials [4]-[7]. Based on the evaluation of various experimental techniques, the measurement of the surface potential decay (SPD) of the corona-charged media has been considered as the most appropriate solution for monitoring the charging state of nonwoven fabrics, because of its simplicity and reliability [8]-[11]. Although, this measurement of the surface potential V_s is widely used for the investigation of the electric charge on dielectric surfaces in a wide range of industry applications, the problem is that most of the literature deals with thin insulating films or with more or less homogenous dielectrics.



Fig. 1. Photograph of the nonwoven polypropylene media.

Several mechanisms are involved in surface potential evolution of such materials: atmospheric neutralization, surface conduction, polarization, intrinsic conduction, piezoelectricity, interfacial charge injection, and so on [11]-[19]. The nonwoven fabrics (Fig. 1) are more difficult to handle, and their physical structure is highly nonhomogeneous at a microscopic and, in many cases, at a macroscopic scale. The corona charging of a nonwoven polypropylene sheet air filter has certain characteristics [20]-[21]: the surface potential of the filter media is limited by the local discharges that occur inside the porous sheet and the relative humidity of the ambient air accelerates the charge decay.

In previous works [4], [22]-[23], the authors employed the SPD technique to evaluate some factors that influence the corona charging of fibrous dielectrics. However, it has been quite difficult to consistently identify the nature of the phenomena involved, since different physical mechanisms can lead to similar responses. The rate of the potential decay dV_s/dt does not account for the initial surface potential V_{s0} , but has the advantage of enabling the identification of these physical processes [11],[19]. Each of them is associated to a peak of different characteristic times and amplitudes on the diagram seconds (tdV_s/dt) versus $(\log t)$.

The aim of this paper is to analyze the behavior of negative corona-charged nonwoven fabrics and to identify the different physical mechanisms that contribute to the SPD. The study was performed on polypropylene nonwoven media under various experimental conditions, such as: corona discharge energy, charging voltage, relative air humidity and thermal conditioning.

II. MATERIALS AND METHODS

The experiments were performed on 60 mm × 50 mm samples of polypropylene nonwoven media (Fig. 1). The media is made of 2.8 dtex PP fibers (average fiber diameter: 20 μm) and its thickness is about 300 μm.

Corona charging and surface potential measurements were done in atmospheric air under various environmental conditions. The samples were placed in contact to the grounded plate electrode (Aluminum, 120 mm × 90 mm). The electrode system was energized from a negative DC high-voltage supply (model SL 300, SPELLMAN; rated voltage: 50 kV; rated current: 6 mA). The corona discharge is generated between a wire-type dual electrode and a metallic grid electrode, which allows the control of surface potential and of discharge energy. The distance between the wire (Tungsten; diameter: 0.2 mm) and the surface of the plate electrode was 30 mm, as shown in Fig. 2. In all the experiments, the samples were charged for 10 second at various grid potentials V_g with a constant current charging characterized by grid current I_g .

As soon as the high-voltage supply of the corona charger was turned-off, a conveyor belt transferred the sample from the charging position to the surface potential measurement positions, shown in (Fig. 3). The transit time between the end of the charging period and the first measured value of the surface potential does not exceed 3 seconds.

The surface potential was measured with an electrostatic voltmeter (TREK, model 341B, equipped with a probe model 3450, accuracy: 0.1% of full scale, drift with temperature 200 ppm/°C), calibrated before each set of measurements. The measured potential was monitored via an electrometer (Keithley, model 6514) connected to a personal computer (Fig. 3). The processing of the data was performed using a virtual instrument in the LabView environment. All the SPD curves are recorded during 15 min.

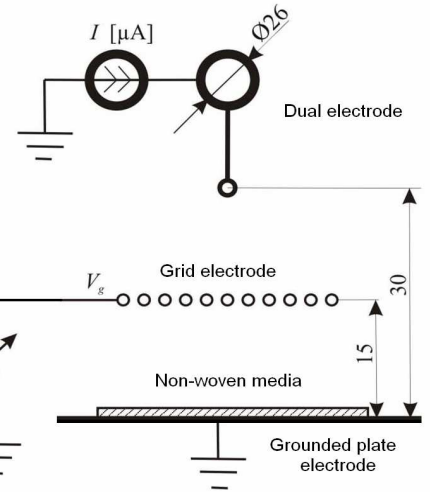


Fig. 2. Electrode systems employed for the corona-charging of non-woven media (all dimensions are in millimeters).

III. RESULTS AND DISCUSSION

The surface potential decay curves of corona charged nonwoven samples and the corresponding (tdV_s/dt) versus ($\log t$) diagrams, are displayed respectively in Figs. 4 and 5, for several values of the grid voltage V_g . The corona charging was performed at the same grid current $I_g = 25 \mu\text{A}$. in atmospheric air, at stable environmental conditions (temperature: 20°C; relative humidity: 65 %).

The absolute value of the initial potential measured at the surface of the corona charged nonwoven fabrics did not exceed 850 V, for all the range of grid voltages (Fig. 4). The limitation of the charging level has two straightforward explanations: (1) the high surface conduction favored by the elevated relative humidity of ambient air; (2) the local discharges that occur inside the fabric, due to the high values of the charging voltage.

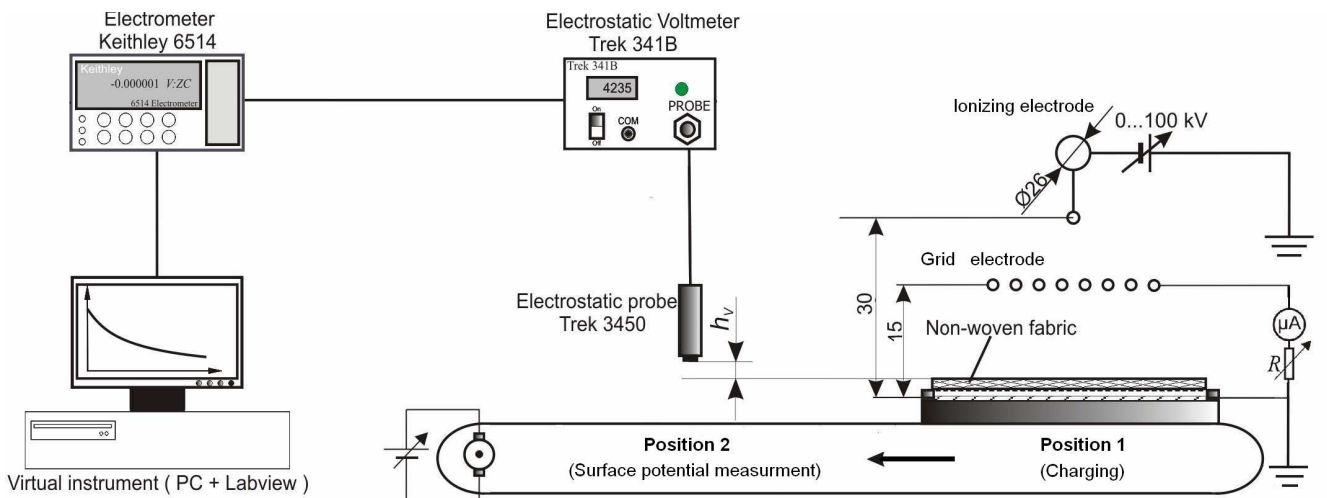


Fig. 3. Experimental set-up for corona charged and SPD measurement on nonwoven fabrics

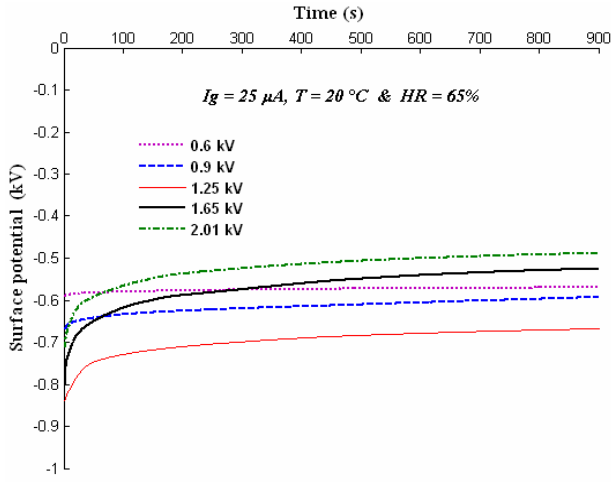


Fig. 4. Surface potential decay curves at several grid voltage values; ($0.6 \text{ kV} \leq V_g \leq 2.01 \text{ kV}$).

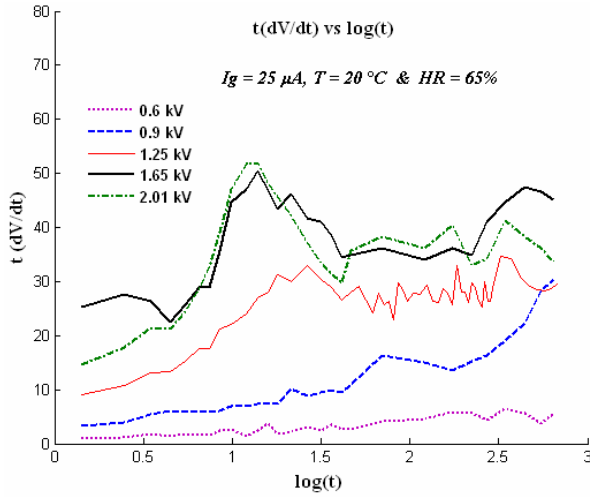


Fig. 5. Plots of $(t(dV/dt))$ curves at several grid voltage values; ($0.6 \text{ kV} \leq V_g \leq 2.01 \text{ kV}$).

For low charging potential V_g values, the decay was very slow. This behavior may be attributed to the fact that the charges deposited on the surface do not have sufficient energy to be freed and injected into the polymer bulk.

At higher V_g , the crossover of the SPD characteristics has been observed, pointing out the existence of a charge injection phenomenon. In the present experiment, the corona discharge energy, which is an activating factor of the injection charge controlled by the air-insulator interface, was low ($I_g = 25 \mu\text{A}$). Therefore, the crossover is probably due to the higher intensity electric field generated in the bulk of the samples by the elevated charge levels initially attained at higher values of the grid voltage V_g . When the charging voltage increase, the potential decay dynamics are characterized by the appearance of a peak centered between 10 s and 101.5 s and its height, which tends to saturate, slightly exceeds 50 (Fig. 5).

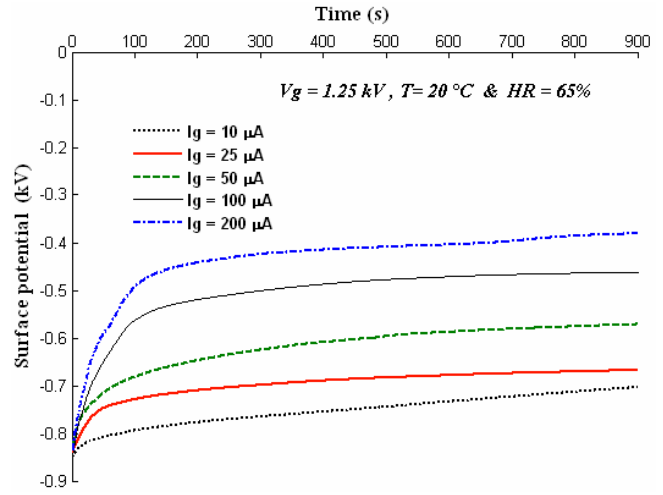


Fig. 6. Surface potential decay curves at several grid current values; ($10 \mu\text{A} \leq I_g \leq 200 \mu\text{A}$).

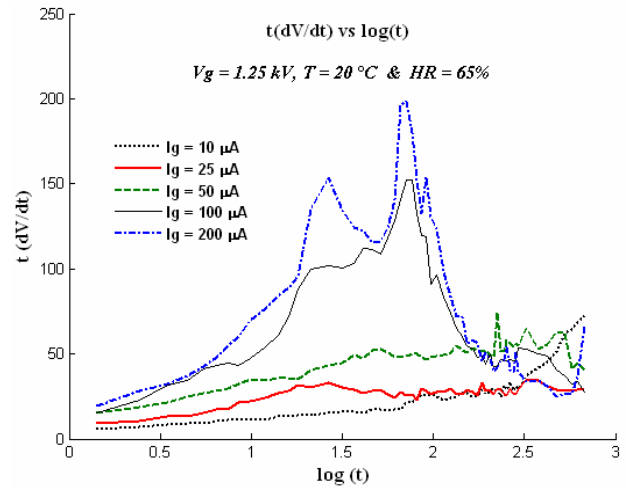


Fig. 7. Plots of $(t(dV/dt))$ curves at several grid current values; ($10 \mu\text{A} \leq I_g \leq 200 \mu\text{A}$).

For low grid voltage value ($V_g = 0.6 \text{ kV}$), the basic dielectric response is linear. This intrinsic response, controlled by the bulk of material, occurs in conditions of moderate values of the two main factors that may activate the charge injection: the electric field and the corona discharge energy. The presence of a peak at higher V_g and low I_g clearly demonstrates that the potential decay dynamics in this experiment depends on the electric field.

To point out the effect of the corona discharge energy on the dielectric response of charged nonwoven fabrics, several experiments were conducted at higher I_g , with the grid voltage maintained at $V_g = 1.25 \text{ kV}$, by acting on the series of calibrated through which the grid is connected to the ground. The initial surface potential measured is virtually the same, however, the decay rate increases when the intensity of the corona discharge increases (Figs. 6 and 7).

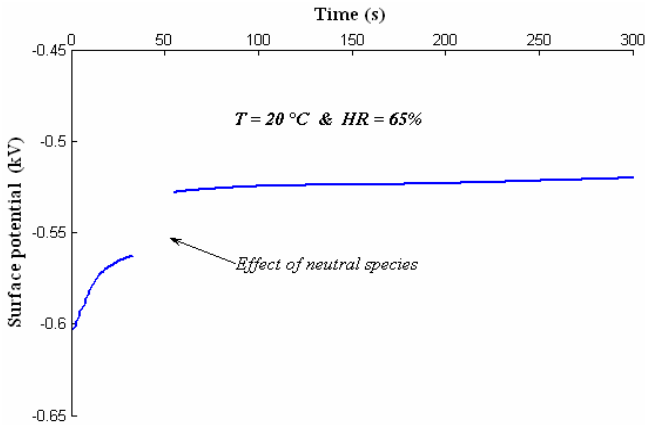


Fig. 8. Effect of exposure to neutral species from a negative corona discharge.

The basic dielectric responses are difficult to identify from diagrams of Fig. 7, even at low grid current values, since the grid voltage is quite high ($V_g = 1.25$ kV). The amplitude of the response ($t(dV_s/dt)$) increases with the corona discharge energy, and this corresponds to the occurrence of broad peaks on the $I_g = 100$ μ A and 200 μ A curves, in the $10^{0.5} - 10^{2.5}$ s time range. The amplitude of this peak did not saturate in the conditions of this experiment; it attained 200 at the highest grid current value.

The SPD dynamics of negative corona-charged nonwoven fabrics is directly related to the discharge energy transferred to the surface. The charge carrier transport processes is linked to the capture and release times from energy traps. However, the charge transit time inside the sample and the releasing mechanism characteristic time are difficult to separate, since the structure of the nonwoven is highly non-homogeneous and the experiments were performed at high relative humidity of the ambient air, which might also affect the SPD dynamics.

In negative polarity, the ions, neutral species and photons are produced during discharge. To verify the influence of the excited neutral species, a corona charged non-woven sample ($V_g = 700$ V, $I_g = 25$ μ A. and $R = 30$ M Ω) is re-exposed after $t = 30$ s to a negative corona discharge, with the grid electrode grounded $V_g = 0$ V, by the closing of the switch K (Fig. 2), and $I_g = 100$ μ A. The SPD curve obtained in this experiment after $t = 30$ s (Fig. 8) shows well that an injection occurs under the action of the neutral excited species generated when the grid was grounded.

Although the electric field and negative corona discharge energy are the main factors of injection activation, it is also useful to evaluate the influence of moisture. The fact that all these factors occur simultaneously complicates the analysis of the response of non-woven materials, the previous experiments having been carried out at high levels of the relative humidity RH of the ambient air. To clarify this issue, SPD measurements were carried out at different RH , for ambient air temperatures close to 20°C and a grid current $I_g = 100$ μ A.

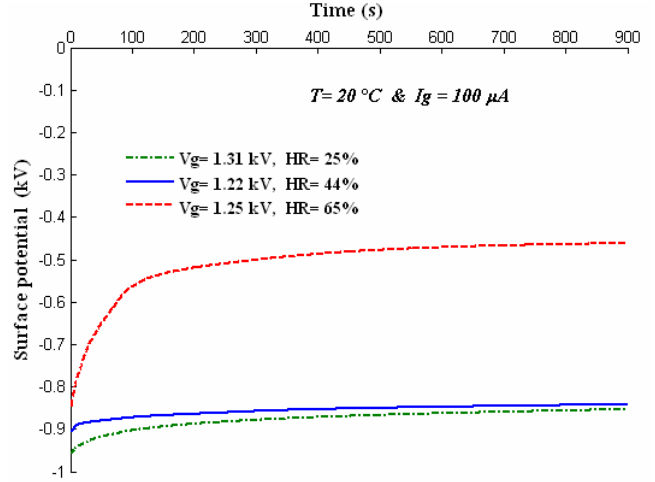


Fig. 9. Surface potential decay curves at several RH values of ambient air.

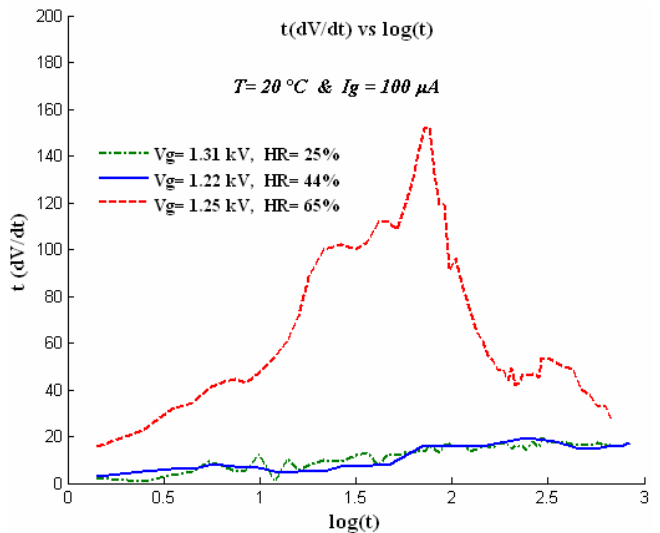


Fig. 10. Plots of $t(dV_s/dt)$ curves at several RH values of ambient air.

The initial surface potential is lower at high RH (Fig. 9); this suggests that the decay is accentuated by surface conduction through the fibrous non-woven fabric. The conduction can occur during both the corona charging and surface potential decay processes. The diagrams ($t(dV_s/dt)$) obtained for $RH = 25\%$ and 44% (Fig. 10) are quite similar. However, when the relative air humidity is 65% , the SPD dynamics are characterized by the occurrence of a broad peak (Fig. 10), in the $10^{0.5} - 10^{2.5}$ s time range (characteristic time closer to 10^2 s). This suggests that the moisture does affect the progression of the charge carriers in the bulk.

Because of the fact that the relative humidity of the ambient air was reduced to 44% , the initial surface potential becomes higher, in spite of a higher level of corona discharge energy ($I_g = 100$ μ A) and exceeds -900 V (Fig. 11) against -830 V for $I_g = 25$ μ A and $RH = 65\%$ (Fig. 4). Also, the diagrams ($t(dV_s/dt)$) shown in Fig. 12, which correspond to $I_g = 100$ μ A and $RH = 44\%$, are different from those recorded at lower $I_g = 25$ μ A and higher $RH = 65\%$ (Fig. 5).

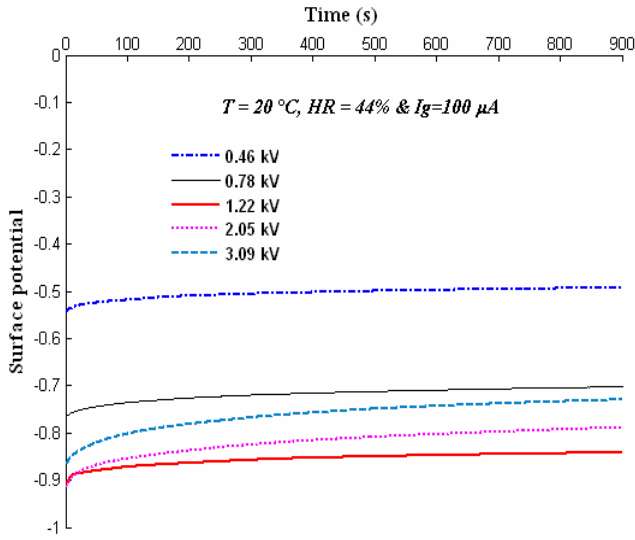


Fig. 11. SPD curves at several grid voltage values and low RH.

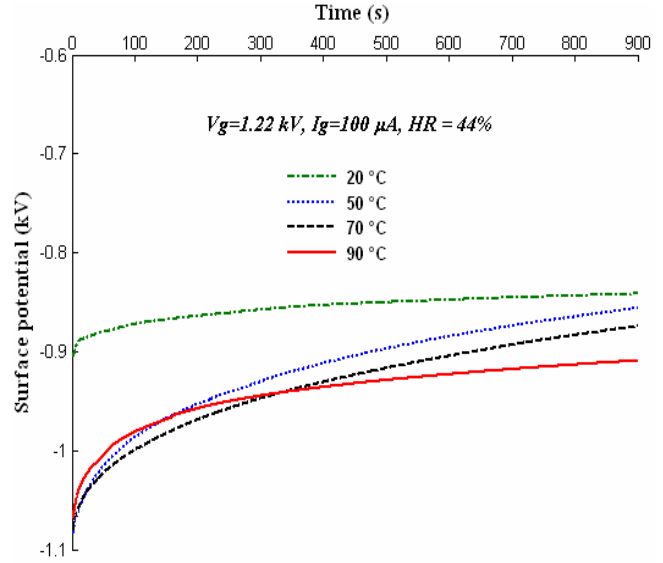


Fig. 13. SPD curves for negative corona-charged non-woven media, after being heated to various temperatures.

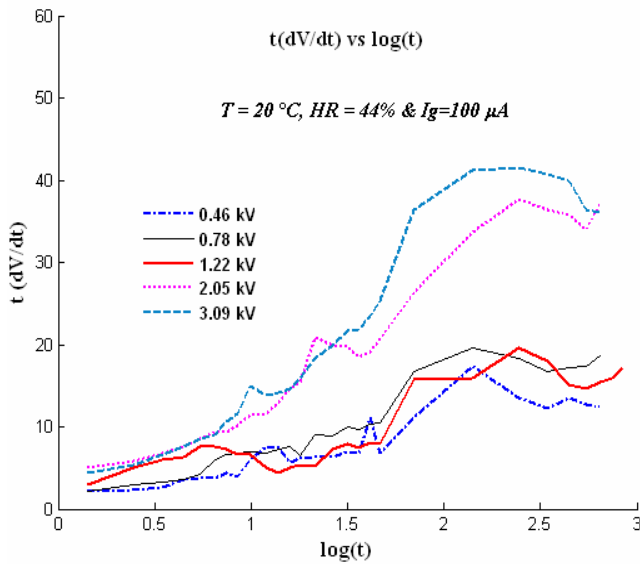


Fig. 12. Plots of (tdV_s/dt) curves at several grid voltage values and low RH.

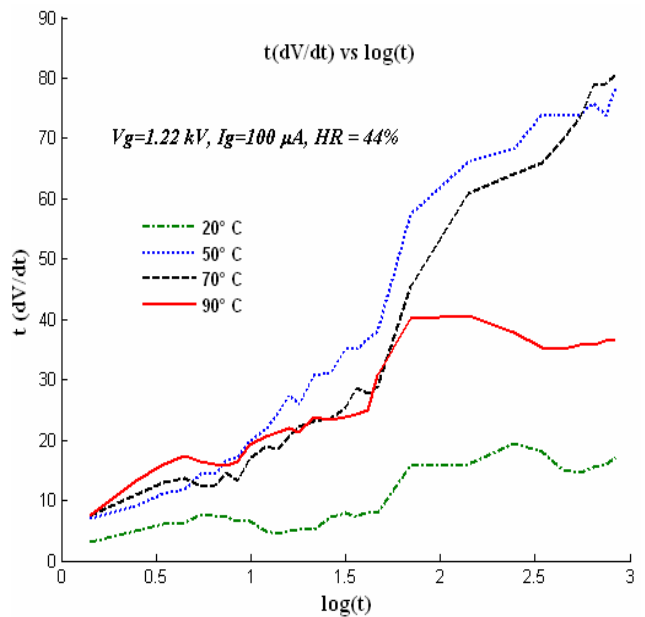


Fig. 14. Plots of (tdV_s/dt) curves for negative corona-charged non-woven media, after being heated to various temperatures.

Heating the samples prior to corona charging changes the aspect of SPD curves and the potential decay dynamics (Figs. 13 and 14). The higher is the temperature at which the samples have been heated, the higher is the initial surface potential (Fig. 13). During the early stage of the SPD curve (i.e., right after stopping the corona charging process), the potential declined faster in the case of samples preheated to higher temperatures. This generates a first crossing of the SPD curves, followed by a second one that occurs at a time when the samples are already cooled and when the decline becomes faster for the samples preheated at lower temperatures. As a consequence, the charging state of the samples preheated at higher temperature becomes more stable and the surface potential is much higher than for the samples preheated at lower temperatures.

The (tdV_s/dt) curves present a low amplitude peak with a characteristic time just above $10^{0.5}$ s. After that first peak, for the samples preheated to 50°C and 70°C, the amplitude increases constantly and no second peak is observed for almost three decades of t .

However, a peak occurs for the samples preheated to 90°C centered above 10^2 s and its amplitude does not exceed 40. This behavior suggest that, during the early stages of the decay, the releasing of the charge injected at the sample surface assisted by negative corona discharge increases with the pre-heating temperature.

The bulk is also involved in the case of the samples preheated at high temperatures, because of the increased number of empty traps. As the temperature decreases with time, this effect vanishes and the SPD slows down. With the charges trapped deeper in the material, the potential is more stable at the surfaces of the samples that have been heated at a higher temperature.

IV. CONCLUSION

The SPD dynamics, characterized by appearance of crossover phenomenon, is caused mainly by two mechanisms, namely charge injection at interfaces and charge transport in the bulk, which are controlled by the trapping and release phenomena. The electric field generated by the charges deposited on the surface of the samples, the energy of the negative corona discharge, and the presence of neutral excited species are significant factors of injection activation. The relative air humidity affects significantly both the initial surface potential and the SPD dynamics. Thermal preconditioning of the nonwoven fabrics improves the charging state. The fact that all these factors occur simultaneously complicates the analysis of the response of such materials.

REFERENCES

- [1] F. J. Rornay, B. Y. H. Liu, and S.-J. Chae, "Experimental study of electrostatic capture mechanisms in commercial electret filters," *Aerosol Sci. Technol.*, vol. 28, pp. 224–274, 1998.
- [2] M. Nifuku, Y. Zhou, A. Kisiel, T. Kobayashi, and H. Katoh, "Charging characteristics for electret filter materials," *J. Electrostat.*, vol. 51/52, pp. 200–205, 2001.
- [3] A. Jaworek, A. Krupa, and T. Czech, "Modern electrostatic devices and methods for exhaust gas cleaning: A brief review," *J. Electrostat.*, vol. 65, pp. 133–155, 2007.
- [4] B. Tabti, M. Mekideche, M. Plopeanu, L. M. Dumitran, L. Herous, and L. Dascalescu, "Corona charging and charge decay characteristics of non-woven filter media," *IEEE Trans. Ind. Appl.*, vol. 46, pp. 634 – 640, 2010.
- [5] J. A. Giacometti, S. Fedosov, and M. M. Costa, "Corona charging of polymers: recent advances on constant current charging," *Brazilian Journal of Physics*, vol. 29, pp. 269–279, 1999.
- [6] R. S. Blacker and A. W. Birley, "Electrostatic charge occurrence, significance and measurement," *Polymer Testing*, vol. 10, pp. 241–262, 1991.
- [7] G.F. Leal Ferreira, D.L. Chinaglia, J.A. Giacometti, and O. N. Oliveira Jr, "Corona triode current-voltage characteristics: on effects possibly caused by the electronic component," *J. Phys. D Appl. Phys.* vol. 28, pp. 528–633, 1993.
- [8] B. Tabti, A. Antoniu, M. Plopeanu, B. Yahiaoui, B. Bendahmane and L. Dascalescu, "Implementation and interpretation of surface potential decay measurements on corona-charged non-woven fabrics," *J. Phys: Conf. Ser.*, vol. 301, no.1, 2040, 2011.
- [9] M.C. Plopeanu, P.V. Notingher, L.M. Dumitran, B. Tabti, A. Antoniu, and L. Dascalescu, "Surface potential decay characterization of non-woven electret filter media," *IEEE Trans. DEI*, vol. 18, pp. 1393 – 1400, 2011.
- [10] A. Antoniu, L. Dascalescu, I.V. Vacar, M.C. Plopeanu, B. Tabti, and H.N. Teodorescu, "Surface potential versus electric field measurements used to characterize the charging state of nonwoven fabrics," *IEEE Trans. Ind. Appl.*, vol. 47, pp. 1118 – 1125, 2011.
- [11] P. Molinié and P. Llovera, "Surface potential measurements: Implementation and interpretation," in *Proc. Dielectr. Mater. Meas. Appl. (IEE Conf. Publ. no. 473)*, pp. 253–258, 2000.
- [12] R. Coelho, "Surface potential decay and return voltage buildup; Applications to the understanding of the electrical transport in insulating films," *5th Int. Conf. Diel. Mater., Measur. & Appl.* (Canterbury, UK), pp. 33 – 36, 1988.
- [13] P. Molinié, "Charge injection in corona-charged polymeric films: Potential decay and current measurements," *J. Electrostat.*, vol. 45, no. 4, pp. 265–273, Feb. 1999.
- [14] A. Crisci, B. Gosse, J-P. Gosse, and V. Ollier-Duréault, "Surface-potential decay due to surface conduction," *Eur. Phys. J. AP*, vol. 4, pp. 107–116, 1998.
- [15] S. Sahli, A. Belle, Z. Ziari, A. Kahlouche, and Y. Segui, "Measure and analysis of potential decay in polypropylene films after negative corona charge deposition," *J. Electrostat.*, vol. 57, pp. 169–181, 2003.
- [16] P. Molinié, "Measuring and modeling transient insulator response to charging: the contribution of surface potential studies," *IEEE Trans. DEI*, vol. 12, pp. 939–950, 2005.
- [17] G. Chen, "Anomalous phenomena in solid dielectrics under high electric fields," *Proc. 9th Int. Conf. Propr. & Appl. Diel. Mater.*, Harbin China, July 19–23, 2009.
- [18] G. Chen, "A new model for surface potential decay of corona-charged polymers," *J. Phys. D: Appl. Phys.*, vol. 43, 055405, 2010.
- [19] P. Molinié and P. Llovera, "New methodology for surface potential decay measurements: application to study charge injection dynamics on polypropylene films," *IEEE Trans. DEI*, vol. 11, pp. 1049–1056, 2004.
- [20] R. Kacprzyk and W. Mista, "Back corona in fabrics," *Fibers Textiles Eastern Eur.*, vol. 14, no. 5, pp. 35–38, 2006.
- [21] T. Oda and J. Ochiai, "Charging characteristics of a non-woven sheet air filter," in *Proc. 6th Int. Symp. Electrets*, Sep. 1–3, pp. 515–519, 1988.
- [22] B. Tabti, L. Dascalescu, M. Plopeanu M, A. Antoniu, and M. R. Mekideche, "Factors that influence the corona charging of fibrous dielectric materials," *J. Electrostat.*, vol. 67, pp. 193–197, 2009.
- [23] B. Tabti, M. Mekideche, M. Plopeanu, L. M. Dumitran, A. Antoniu, and L. Dascalescu, "Factors that influence the decay rate of the potential at the surface of non-woven fabrics after negative corona discharge deposition," *IEEE Trans. Ind. Appl.*, vol. 46, pp. 1586 – 1592, 2010.